Proceedings of the Combustion Institute

Subgrid modeling of intrinsic instabilities in premixed flame propagation

--Manuscript Draft--

Manuscript Number:	
Article Type:	4. Laminar Flames
Keywords:	Intrinsic flame instability; Darrieus-Landau instability; Thermal-diffusive instability; Direct Numerical Simulation; Wrinkling factor.
Corresponding Author:	Pasquale Eduardo Lapenna, Ph.D. Rome, ITALY
First Author:	Pasquale Eduardo Lapenna, PhD, Research Associate
Order of Authors:	Pasquale Eduardo Lapenna, PhD, Research Associate
	Rachele Lamioni, PhD Student
	Francesco Creta, Associate Professor
Abstract:	This work is devoted to the investigation and subgrid-scale modeling of intrinsic flame instabilities occurring in the propagation of a deflagration wave. Such instabilities, of hydrodynamic and thermodiffusive origin, are expected to be of particular relevance in recent technological trends such as in the use of hydrogen as a clean energy carrier or as a secondary fuel in hydrogen enriched combustion. A dedicated set of direct numerical simulations is presented and used, in conjunction with coherent literature results, in order to develop scaling arguments for the propagation speed of self-wrinkled flames which are also supported by the outcomes of a weakly non-linear model. The observed scaling is based on the number of unstable wavelengths in a planar flame and is used to develop an algebraic model for the wrinkling factor in the context of a flame surface density closure approach. An a-priori analysis shows that the model correctly captures the flame wrinkling caused by intrinsic instability at sub grid level. A strategy to include the developed self-wrinkling model in the context of a turbulent combustion model is finally discussed on the basis of the turbulence induced cut-off concept.

Subgrid modeling of intrinsic instabilities in premixed flame propagation

Pasquale Eduardo Lapenna[ab], Rachele Lamioni[a], Francesco Creta[a]

[a] *Dept. of Mechanical and Aerospace Engineering, Sapienza University of Rome, Italy*
[b] *ENEA C.R. Casaccia, via Anguillarese 301, Rome, Italy*

Abstract

This work is devoted to the investigation and subgrid-scale modeling of intrinsic flame instabilities occurring in the propagation of a deflagration wave. Such instabilities, of hydrodynamic and thermodiffusive origin, are expected to be of particular relevance in recent technological trends such as in the use of hydrogen as a clean energy carrier or as a secondary fuel in hydrogen enriched combustion. A dedicated set of direct numerical simulations is presented and used, in conjunction with coherent literature results, in order to develop scaling arguments for the propagation speed of self-wrinkled flames which are also supported by the outcomes of a weakly non-linear model. The observed scaling is based on the number of unstable wavelengths in a planar flame and is used to develop an algebraic model for the wrinkling factor in the context of a flame surface density closure approach. An a-priori analysis shows that the model correctly captures the flame wrinkling caused by intrinsic instability at sub grid level. A strategy to include the developed self-wrinkling model in the context of a turbulent combustion model is finally

Email address: pasquale.lapenna@uniroma1.it, pasquale.lapenna@enea.it, pasquale.lapenna@gmail.com (Pasquale Eduardo Lapenna[a])

discussed on the basis of the turbulence induced cut-off concept.

Keywords: Intrinsic flame instability; Darrieus-Landau instability; Thermal-diffusive instability; Direct Numerical Simulation; Wrinkling factor.

Paper length: 6.5 pages including reference according to the two-column format.

Colloquium 1: Laminar Flames

Colloquium 2: Turbulent Flames

1. Introduction

Intrinsic instabilities appear in premixed flames in different forms and scales [1]. The two intrinsic mechanisms are the Darrieus-Landau (DL) or hydrodynamic instability caused by the thermal expansion and the thermodiffusive (TD) instability generated by unbalanced heat and mass fluxes in the reaction region [2–4]. While the former is ubiquitous and always destabilizing, the latter can be either stabilizing or destabilizing depending on the effective Lewis number of the controlling reactant [5]. The DL instability can only develop for large-scale flames as the scale of its induced wrinkling is typically two orders of magnitude larger than flame thickness in both laminar as well as turbulent settings [6]. The DL features have been studied both experimentally [7–9] and numerically, employing techniques ranging from weakly non-linear models to direct numerical simulations (DNS) [10–13]. Conversely, TD instability manifests itself typically in lean hydrogen flames, with small scale cellular structures on the order of some flame thicknesses as shown by DNS [14–17] as well as experiments [18, 19].

From a phenomenological standpoint, a flame which is intrinsically unstable, tends to propagate faster than its corresponding stable case. The DL or TD induced corrugations in its nonlinear evolution tends to increase the instantaneous flame area and therefore the mean propagation of the entire flame front creating a self-turbulent propagation regime, even in the absence of any incoming turbulence [20]. The modeling of the self-wrinkling behavior as well as the interplay of instabilities and turbulence still require a substantial research effort. In fact, state-of-the-art premixed combustion models do not include any instability-related parameter: see for instance the discussion

on flame surface density (FSD) in [6]. Nevertheless, some attempts have been made, in the context of sub grid scale (SGS) modeling for large eddy simulations (LES) of unconfined deflagration [21] and Bunsen flames[22].

This being said, the investigation of intrinsic instability is nowadays also of practical importance, being motivated by recent technological trends such as the increasing operating pressure of combustion chambers as well as the use of hydrogen as a clean energy carrier or as a secondary fuel in hydrogen enriched flames. These conditions are expected to promote the occurrence of both TD and DL instability [23–26], creating challenging conditions to model turbulent premixed combustion, which can lead to non-predictive results from standard approaches: see for instance [27]. In this framework, the present work aims at the analysis and modeling of the flame wrinkling ensuing from intrinsic flame instabilities. To this end, a DNS dataset consisting of two series of flames influenced by DL and TD instability is developed without any turbulent forcing. The ensuing mean propagation speeds, in conjunction with similar results from recent DNS works [13–15], are used to develop an algebraic wrinkling factor model. Such model is tested in an a-priori fashion following [28]. Finally the possibile inclusion of the model into turbulent combustion closure based on the FSD concept, is discussed.

2. Theoretical and numerical framework

2.1. The lengthscales of intrinsic instabilities

In the context of intrinsic instabilities, linear stability analysis of a planar flame is a viable technique to estimate the lengthscales at play. The ensuing dispersion relation $\omega(k)$, where ω is the growth rate of a small perturba-

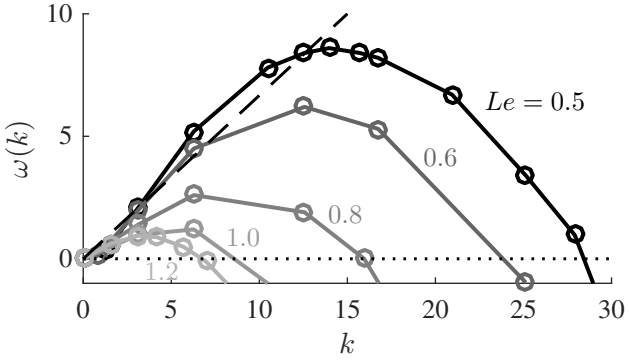

Figure 1: Lewis number effect on the dispersion relation

tion of wavelength λ and wavenumber $k = 2\pi/\lambda$, furnishes two reference lenghtscales, namely the cutoff (or neutral) wavelength $\lambda_c = 2\pi/k_c$, where $\omega(k_c) = 0$ and the most unstable wavelength λ_{max} for which $d\omega/dk = 0$. Such lenghtscales as well as the shape of $\omega(k)$ are largely influenced by the Lewis number of the fuel Le as shown in Fig. 1, in which dispersion relations have been obtained numerically by means of DNS, using the approach described later. As Le decreases, k_c becomes larger and around $Le \approx 0.6$, the dispersion relation exhibits an overshoot above the linear behavior representing the DL mechanism. This indicates that below a critical Lewis number Le_0, thermal-diffusive effects are destabilizing for the flame front [5]. For $Le > Le_0$ i.e. when thermal-diffusive effects are stabilizing, dispersion relations can be either reconstructed numerically by means of DNS or determined analytically using variable fidelity hydrodynamic models [4, 5]. Conversely, for $Le < Le_0$ i.e. for destabilizing thermal-diffusive effects, analytical models are not available and $\omega(k)$ can only be obtained numerically as in Fig. 1.

As discussed in [6], λ_c thus acquires the meaning of a characteristic flame lengthscale, on equal footing with flame thickness to be compared to tur-

bulence lenghtscales. Indeed λ_c is uniquely defined by the thermochemical conditions, such as the unburned flame temperature T_u, background pressure p_0 and mixture ratio ϕ. A measure of the degree of instability is given by $n_c = L/\lambda_c$, the number of unstable wavelengths within a reference hydrodynamic length L, which is assumed as the largest lengthscale constraining the flame. The higher the value of $n_c > 1$, the larger the number of unstable cells and the more severe the corrugation of the flame is to be expected.

2.2. DNS datasets

Intrinsically unstable flames are typically very large scale flames [6] and their DNS requires long simulation times [15]. The computational cost of large scale flame simulations is elevated even in 2D settings with simple chemistry, which are indeed used in this work. In order to have a dataset capable of sustaining scaling arguments with good confidence, we employ, in addition to our DNS data, coherent results from other groups. Our simulations employ a well established framework [6, 29–31], based on the low-Mach number approximation and on a deficient reactant controlling a one-step irreversible reaction. This approach is implemented in an equation-of-state-independent version [32–35] of the highly-efficient parallel code *nek5000* [36] based on the spectral element method (SEM) [37].

Two series of planar flames have been simulated, designated TD and DL to highlight respectively the presence or absence of thermal-diffusive instabilities, with increasing values of n_c. For each simulation λ_c, needed to determine n_c, has been evaluated numerically and, where possible, compared to analytical dispersion relations [5]. The computational domain is periodic in the crosswise direction while outflow conditions are imposed at the up-

Table 1: Summary of DNS parameters and characteristics.

Label	Le	σ	Ze	n_c	L/ℓ_D	S_T/S_L^0
DL1	1.36	10.0	8.0	9.2	400	1.57
DL2	1.00	6.67	8.0	13.7	400	1.32
DL3	1.00	10.0	8.0	16.3	400	1.85
TD1	0.49	6.67	8.0	7.6	40	2.03
TD2	0.49	6.67	8.0	20.0	105	4.03
TD3	0.49	6.67	8.0	76.0	400	4.52

per boundary in the streamwise direction. Statistically planar flames are obtained by means of an inflow/outflow configuration, imposing the instantaneous burning velocity as the inflow velocity at the lower boundary [38] without introducing any turbulent perturbation. The SEM discretization is uniform and the resolution chosen in order to have, for the less resolved case, at least 14 grid points within the thermal thickness of a 1D unstretched flame, defined as $\delta_T = (T_b - T_u)/\max(dT/dx)$. The simulations are initialized by means of a 1D flame with the superimposition of a small broadband velocity disturbance to trigger the instability and statistics are collected only after reaching the non-linear regime.

The TD series is characterized by a ratio between the domain width and the flame thickness L/ℓ_D ranging from 40 up to 400, resulting in a wide range of n_c. The size of the computational domain in the streamwise direction L_y is two times the periodic dimension L, which was verified to be large enough to correctly contain the corrugated flame for the entire non-

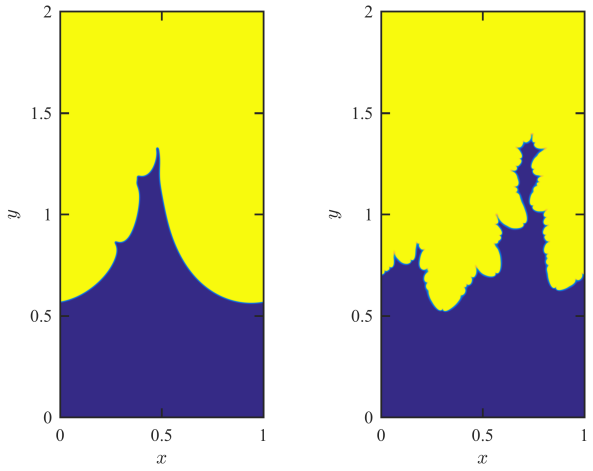

(a) DL3 (b) TD3

Figure 2: Progress variable fields for the largest flames of the dataset. Color code from blue ($c = 0$ unburnt) to yellow ($c = 1$ burnt).

linear evolution studied. Conversely, the DL series is obtained by varying both the expansion ratio σ and the Lewis number Le while keeping constant $L/\ell_D = 400$. In this series a computational domain in the streamwise direction of $L_y = L$ was deemed large enough, except for the simulation labeled as DL3 in which $L_y = 2L$. As a result, being λ_c larger in units of ℓ_D for thermal-diffusively stable flames, the range of n_c that can be explored by the DL series using similar computational resources is clearly narrower than the TD series. A summary of the DNS parameters is reported in table 1 in conjunction with the mean propagation speeds S_T/S_L^0 while instantaneous realizations of the largest flames, namely TD3 and DL3, are displayed in Fig. 2. We also employ literature data from other recent DNS simulations of two-dimensional, self-turbulent flames. In particular, mean propagation speed of statistically planar flames are taken from the following: (i) Yu et

al. [13], hydrodynamically unstable one-step chemistry flames with $Le = 1$, $\sigma = 5, 8, 10$ and $n_c = 1 - 95$; (ii) Berger et al. [15], TD unstable, lean hydrogen flames ($\phi = 0.44$) at an estimated effective Lewis number of $Le = 0.39$ and $\sigma = 4.4$ data taken only in the range $n_c = 2 - 300$; (iii) Frouzakis et al. [14], TD unstable lean hydrogen flames ($\phi = 0.5$, estimated $Le = 0.53$ and $\sigma = 5$) in the range $n_c = 2 - 4$.

3. Results and discussion

3.1. Analysis and modeling of self-wrinkling

Phenomenologically, the self wrinkling caused by intrinsic flame instability is associated to a flame area increase responsible for the overall flame speed enhancement. Any attempt to model such wrinkling should involve the determination of a scaling law for S_T/S_L^0 and the adequate set of independent parameters governing it. Valuable information can be obtained from the Sivashinsly equation [39], modeling the unsteady perturbation $u(x,t)$, about the nominal planar conformation, of a potentially hydrodynamically and thermodiffusively unstable flame with weak thermal expansion. The integrodifferential model in a periodic domain of size L is originally cast as a function of the expansion ratio σ and of a parameter ϵ measuring the deviation of the Lewis number from the critical value Le_0. This can be reduced through variable transformation to a one parameter equation in one spatial dimension:

$$u_t + u_{xxxx} + \beta u_{xx} + 1/2 u_\xi^2 = I(u) \tag{1}$$

where β is the only surviving parameter and $I(u)$ is the non-local Hilbert transform of the derivative of u representing thermal expansion effects. As

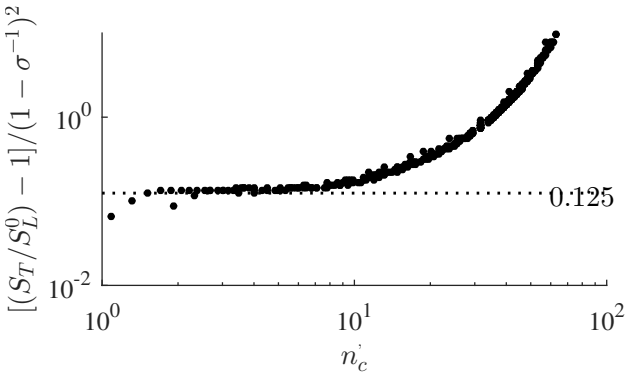

Figure 3: Incremental propagation speed obtained averaging the solutions of the Sivashinsly equation.

β is varied, the enhanced propagation speed of a cellular flame, solution of the model, is obtained by time averaging the flame area. Noting that the associated dispersion relation depends on the unique parameter β, so will the suitably rescaled cutoff wavelength λ_c' and rescaled number of unstable wavelengths n_c'. One thus expects the averaged propagation speed to exhibit a universal scaling law as a function of n_c'. This is indeed the case as shown in Fig. 3 displaying, for a large number of solutions, the incremental propagation speed $[(S_T/S_L^0)-1]$ rescaled by $(1-\sigma^{-1})^2$ to compensate for thermal expansion which tends to increase the amplitude of corrugations. For small values of $n_c' > 1$ one observes flame conformations similar to *pole* solutions (0.125 asymptotic value) [40] typical of DL instability, while for larger n_c' additional wrinkling due to growing effects of TD instability further increases the propagation speed.

On the basis of the indications gleaned through the Sivashinsky model, it is reasonable to scale the averaged burning velocity from the DNS database as a function of: (i) n_c, as a measure of the degree of intrinsic instability and

(ii) σ, to account for the effect of thermal expansion on the amplitude of the corrugation. To compensate for thermal expansion, we employ this time the function $U_m(\sigma)$, in lieu of $(1-\sigma^{-1})^2$, derived for realistic values of σ by Bychkov [41], representing the incremental propagation speed of a corrugated stationary flame subject to DL instability. Such function, was verified against dedicated DNS data, although we do not show this for brevity. Figure 4 finally shows the rescaled incremental propagation speed $(S_T/S_L^0-1)/U_m$, as a function of n_c. It is clearly noticeable that flames influenced by TD instability propagate faster, for a given n_c, than the purely hydrodynamically unstable flames. The latter ($Le > Le_0$) seem to follow reasonably well the analytical incremental propagation speed of pole solutions $U_N(n_c) = \frac{1}{2}\frac{N}{n_c}(1-\frac{N}{n_c})$ with $N = \mathrm{int}(n_c/2+1/2)$ [41]. This trend remains valid up to a secondary cut-off limit, that can be identified between n_c values of 4-4.5 [42] and 7-8 [13], when the well-known global steady DL structure becomes again unstable as the large scale flame starts behaving as a set of quasi-planar, smaller scale unstable flames [42] exhibiting additional wrinkling and a fractal conformation [13, 40]. This additional wrinkling is also present in the simulations DL1-3 from this study, and clearly shown for DL3 case in Fig.2. However, in the case of extremely large domains L, namely more than 2 orders of magnitude larger than λ_c ($n_c > 100$), it is still unclear if a domain independence will be reached. Conversely, for TD unstable flames ($Le < Le_0$) a plateau is reached beyond $n_c \sim 30$ with the largest DNS presented in this work, namely the TD3 case shown in Fig. 2 that confirms the trend recently explained by Berger et al. [15]. On the other hand smaller flames, $n_c \sim 2-30$, show a steady increase before reaching the mentioned plateau.

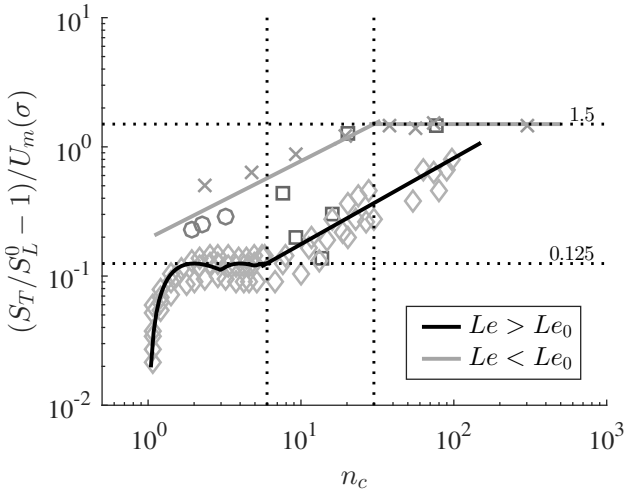

Figure 4: Rescaled incremental propagation speed $(S_T/S_L^0 - 1)/U_m$ plotted against n_c: diamonds ($\diamondsuit$) Yu et al. data [13], crosses ($\times$) Berger et al. data [15], circles ($\bigcirc$) Frouzakis et al. data and squares ($\square$) this study. Continuos lines represent wrinkling factor models in the presence of intrinsic instability for TD and DL cases.

The foregoing observations on propagation speed in the presence of intrinsic instabilities suggest a possible modeling strategy in the context of the generalized FSD approach [43]. The generalized FSD $\Sigma_{\text{gen}} = \overline{|\nabla c|}$ can be modeled by introducing an algebraic expression for the wrinkling factor $\Xi = \overline{|\nabla c|}/|\nabla \overline{c}|$, representing the effect of subgrid wrinkling [28, 43]. In the present context of laminar, self-corrugated, unstable flames, the wrinkling factor can be directly related to flame speed, i.e. $\Xi_L \sim S_T/S_L^0$. This suggests that the rescaled propagation speed of Fig. 4 can be used directly to model the wrinkling factor in a data-driven fashion. Indeed we can conjecture that in a generic setting of turbulent propagation, the overall wrinkling factor Ξ will be a function of both the intrinsic laminar wrinkling Ξ_L and the standard contribution of the turbulent wrinkling Ξ_T. The continuous lines shown in

Fig. 4, fitting the DNS data with a $\sim 20\%$ mean error, can thus effectively represent the model $\Xi_L \sim S_T/S_L^0$, as summarized in Tab. 2.

Table 2: Wrinkling factor model Ξ_L for TD and DL flames.

Le range	n_c range	model expression
any	$n_c < 1$	$\Xi_L = 1$
$Le > Le_0$	$n_c < 6$	$\Xi_L = 1 + U_m(\sigma)(U_N(n_c))$
	$n_c > 6$	$\Xi_L = 1 + U_m(\sigma)(.04 n_c^{2/3})$
$Le < Le_0$	$n_c > 1$	$\Xi_L = 1 + U_m(\sigma)(.19 n_c^{3/5})$
	$n_c > 30$	$\Xi_L = 1 + U_m(\sigma)(1.5)$

Note that for $n_c < 1$ all models should collapse on $\Xi_L = 1$ as the flame is stable within the hydrodynamic domain of interest. Different ranges on n_c are introduced due to the additional cut-off values previously discussed for both TD and DL instability.

The concept of n_c in the context of SGS models should be further explored. The definition of $n_c = L/\lambda_c$ expresses the number of unstable wavelengths within the hydrodynamic length L. In a RANS context, where all the instability-induced wrinkling is unresolved, we should consider L as being the reference hydrodynamic length (e.g. a Bunsen or injector diameter). As a result, n_c is generally expected to be large, thus yielding correspondingly non-unity values of Ξ_L. On the other hand, in an LES context, a portion of the wrinkling may well be resolved on the grid, implying that the hydrodynamic length should be considered as the local grid size $L = \Delta$ so that $n_c = \Delta/\lambda_c$. For $Le > Le_0$ mixtures (such as rich hydrocarbon mixtures), λ_c

can be assumed to be of the order of 10^2 flame thicknesses [6], thus making it extremely likely that $n_c = O(1)$ or less (unless $\Delta > 10^2$ flame thicknesses or larger), thus not requiring any modeling. Conversely, for $Le < Le_0$ (such as lean hydrogen mixtures) λ_c is generally far smaller and can be assumed to be of the order of $10\delta_T$ or less [15], such as in the present TD series of DNS where $\lambda_c \sim 4\delta_T$. This entails a possible value for $n_c > 1$ if the LES filter width is some flame thicknesses wide, which is a far more likely scenario. This reasoning shows that LES of hydrogen or hydrogen-diluted flames may likely require SGS modeling for the unresolved instability-induced wrinkling as confirmed by the a-priori analysis in the next subsection. This being said, whether in a RANS or LES context, a global or local value of n_c should invariably be determined, for the given fuel mixture and given geometry or grid. A good practice would thus require the determination of λ_c for the given mixture and conditions, by numerically determining the flame's dispersion relation.

3.2. A priori analysis of the proposed model

The proposed modeling strategy based on Ξ_L, is now a-priori tested by filtering DNS data using a Gaussian shaped kernel. The overbar $\bar{\cdot}$ denotes LES filtering and the assessment of the FSD based modeling strategy follows standard criteria [28]: (1) the total modeled flame surface area, i.e. the volume-averaged generalized FSD $\langle \Sigma_{gen} \rangle$, should be equal to the DNS value and as independent as possible from Δ; (2) the statistical correlation between the modeled Σ_{gen} and the DNS value should be close to unity, (3) the model should be able to capture the correct variation of conditionally averaged values of Σ_{gen} with filtered reaction progress variable across the flame brush.

The two largest simulations of the dataset, namely DL3 and TD3, are filtered using a wide range of filter sizes from $\Delta = \Delta_{DNS}$ up to $\Delta = 40\delta_T$.

Figure 5 displays the capabilities of $\Sigma_{gen} = \Xi_L|\nabla\overline{c}|$ of reproducing the total flame surface area obtained from the DNS (criterion 1). An overall agreement between the model and the DNS data is observed. In the DL case, the model shows an under-prediction throughout the filter sizes explored. In particular we have $\Xi_L = 1$ until $\Delta \sim \lambda_c \sim 13\delta_T$ where n_c becomes greater than unity. For $\Delta/\delta_T > 13$ the wrinkling factor $\Xi_L > 1$ reduces the difference between $\Xi_L|\nabla\overline{c}|$ and the DNS value. Note that, even for the largest filter size $\Delta/\delta_T \sim 40$, the second part of the model, which activates for n_c greater than the secondary cut-off, was never utilized. Such region would have been explored if Δ were large enough to accommodate at SGS level a large enough flame to exhibit a fractal-like wrinkling. However, such large size filters, compared to the instability and flame lengthscales, cannot be expected in a turbulent scenario as this would imply unrealistically low-Karlovitz numbers, see e.g. Fig.2 of [6]. In the TD case, the model activates at a smaller Δ, around $\Delta/\delta_T \sim 4$, causing a temporary over-prediction of $\langle\Sigma_{gen}\rangle$ until $\Delta/\delta_T \sim 13$. To some extent, this is a good scenario for the interaction between modeling strategies and numerical errors in LES [44]. In addition, the largest filter size $\Delta/\delta_T \sim 40$ is characterized by $n_c \sim 12$ and, as a result, also in this case the second part of model has not been explored. Nonetheless, contrary to DL flames, for TD unstable flames the plateauing region of the Ξ_L model could be realistically used in an LES of a sufficiently large scale flame.

In order to further test the model we now focus on three filter sizes $\Delta/\delta_T \sim$

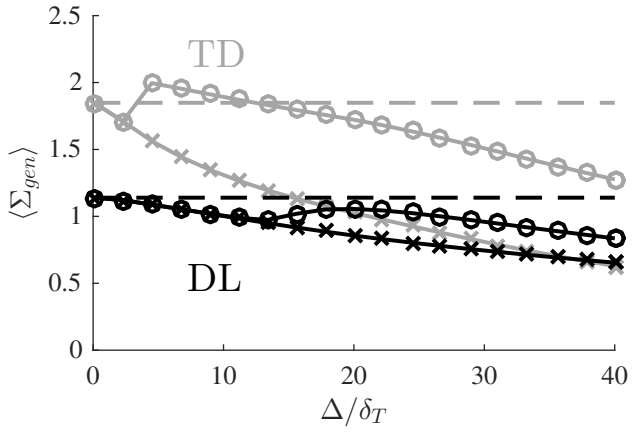

Figure 5: Total volume-averaged value of the generalized FSD as a function of the filter width: DNS value (dashed lines, $--$), modeled Σ_{gen} (circles, $\bigcirc$) and resolved part of the FSD $|\nabla \overline{c}|$ (crosses, $\times$).

$5, 15, 30$ namely fine, medium and coarse. The effect of Δ on c-fields of the TD3 and DL3 cases are shown in Fig.6. It is clearly observable that the secondary wrinkling of the DL case is resolved on the fine grid while for the coarse it is undetectable as the only structure resolved is the large scale DL cusp. In the TD case, the small scale wrinkling is barely visible on the fine grid and undetectable on others, conversely large scale flame fingers are resolved on both fine and medium grids, while at the largest Δ it starts being undetected. As a partial conclusion, in an LES setting, large scale features of both TD and DL type flames can be considered always resolved on the computational grid.

The model is further assessed by investigating the conditionally averaged values of Σ_{gen} to $\overline{c}$ (criterion 3). These quantities are displayed in Fig. 7 showing that the model can reproduce both in shape and magnitude the DNS data. Moreover, Fig. 7 also reports the correlation coefficient between

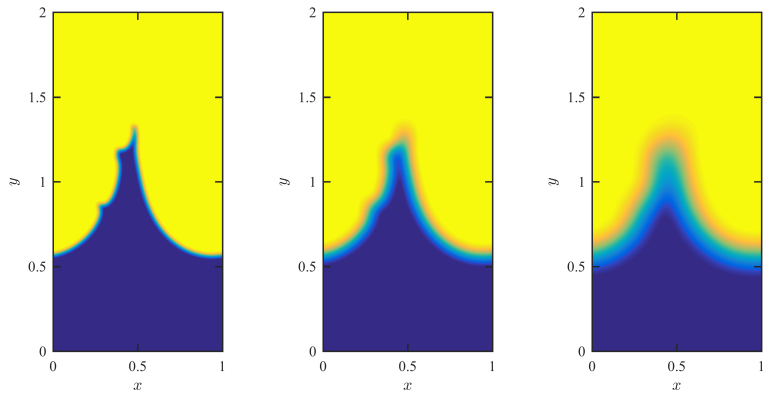

(a) DL3, fine (b) DL3, medium (c) DL3, coarse

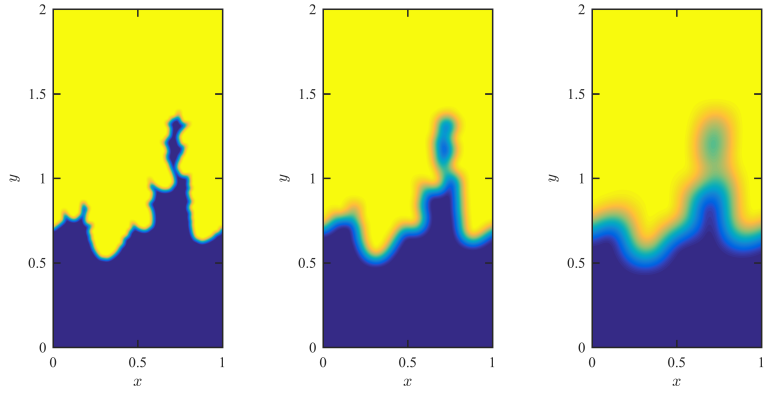

(d) TD3, fine (e) TD3, medium (f) TD3, coarse

Figure 6: The effect of filtering on the instantaneous realizations displayed in Fig. 2: left column TD3 case, right column DL3 case.

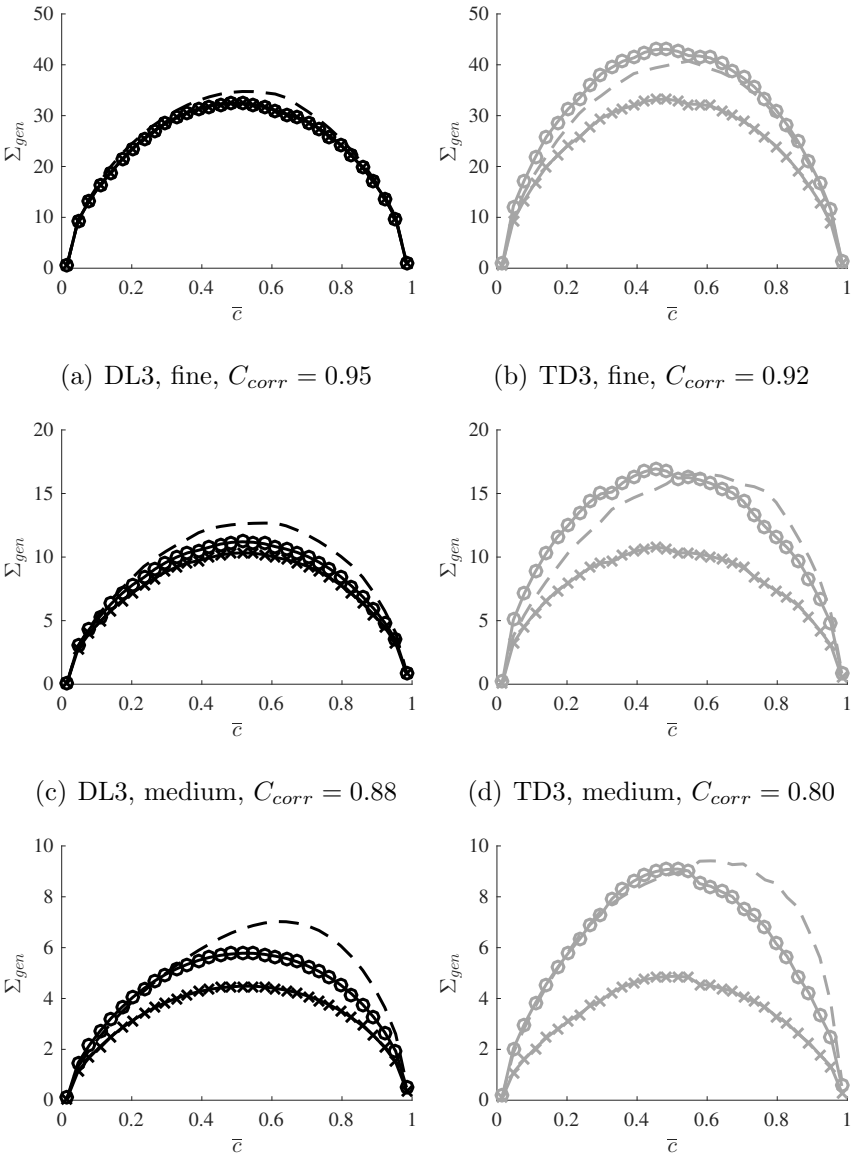

(a) DL3, fine, $C_{corr} = 0.95$ (b) TD3, fine, $C_{corr} = 0.92$

(c) DL3, medium, $C_{corr} = 0.88$ (d) TD3, medium, $C_{corr} = 0.80$

(e) DL3, coarse, $C_{corr} = 0.79$ (f) TD3, coarse, $C_{corr} = 0.72$

Figure 7: Conditionally averaged values of $\Sigma_{gen} = \Xi_L |\nabla \overline{c}|$ to $\overline{c}$, using the three filters $\Delta/\delta_T \sim 5, 15, 30$ namely fine, medium and coarse: DNS (dashed lines, $--$), modeled Σ_{gen} (circles, $\bigcirc$) and resolved part of the generalized FSD $|\nabla \overline{c}|$ (crosses, $\times$). Also reported for each case the correlation coefficient C_{corr} between the exact and modeled Σ_{gen}.

the modeled Σ_{gen} and DNS values (criterion 2), which remain sufficiently close to unity. For the DL flame, Fig. 7(a) and 7(c) statistically confirm the conclusions drawn by observing the $\overline{c}$ fields as $\Xi_L \to 1$ for the medium and fine grid. Only using a large Δ, Ξ_L is appreciably higher than unity and its effect on Σ_{gen} clearly visible. Indeed, for such filter size, the secondary DL structures are statistically not resolved on the mesh. On the other hand, in this case the Σ_{gen} of the DNS is slightly skewed towards the burnt gas side and not perfectly reproduced by the model for $\overline{c} > 0.4$. For the TD flame, the scenario is completely different since the small scale wrinkles require modeling in both the medium and fine grids and the model correctly captures the DNS data across the entire flame brush. In the coarse mesh case, similarly to the DL flame, the exact Σ_{gen} is slightly skewed toward $\overline{c} = 1$ and the model perfectly reproduces the DNS data for $\overline{c} < 0.5$.

3.3. Extension to the turbulent case

A final note is dedicated to the extension of the model of Tab. 2 to a realistic turbulent scenario. Indeed, we recall that such model was derived in a self-wrinkling setting and its characteristics may vary in a turbulent scenario. Previous studies have shown [29, 31], albeit limited to $Le > Le_0$, that for increasing turbulence intensity, the effects of instability-induced wrinkling tend to be mitigated. This may suggest that at high turbulence intensity, the model may have a reduced or even vanishing effect ($\Xi_L \to 1$). Therefore, to tentatively introduce the mitigation of instability, it is of interest to use the concept of turbulence-induced DL cutoff $\tilde{\lambda}_c$, a function of turbulence and instability parameters [42].

A simple way to incorporate turbulence effects is to define a *turbulent* n_c

based on the filter size and $\tilde{\lambda}_c$ as $\tilde{n}_c = \Delta/\tilde{\lambda}_c$. The overall wrinkling factor model can be expressed as $\Xi = \Xi_L(\tilde{n}_c, \sigma)\Xi_T$ where $\Xi_L(\tilde{n}_c, \sigma)$ is the model of Tab. 2 using $\tilde{n}_c$ in lieu of the laminar value, while Ξ_T is a standard model for turbulent premixed combustion. In the limit case of a laminar setting $\tilde{n}_c \to n_c$ while for elevated turbulence intensity $\tilde{n}_c \to 0$ resulting in $\Xi_L = 1$. This being said, the effectiveness of this extension is based on a proper estimation of $\tilde{\lambda}_c$ that defines $\tilde{n}_c$ on the LES grid. While for DL flames the definition in [42] could be tested, for TD flames it still remains to be investigated/proposed. It is not known, in fact, whether this mitigation effect will also occur for $Le < Le_0$, where it may be delayed by the small scale and persistent nature of thermal-diffusive corrugations.

4. Conclusion

The propagation of intrinsically unstable flames has been investigated and a model to incorporate the possibile occurrence of instability-induced wrinkling at subgrid level has been introduced. The model is based on scaling arguments of the average propagation speed as a function of the number of unstable wavelengths for a planar premixed flame n_c. The scaling has been sustained by the results of a weakly non-linear model and by the development of a dedicated DNS dataset as well as other coherent literature results. In particular, purely hydrodynamically unstable flames seem to exhibit incremental propagation speeds which follow quite well analytical pole solutions until reaching the secondary cut-off value beyond which additional wrinkling appears. Conversely, thermodiffusively unstable flames show a different scaling with n_c leading to incremental propagation speeds which

are larger than for the corresponding purely hydrodynamic case, eventually reaching a plateau at a large scale cut-off value. The ensuing data have been used to introduce an algebraic model for the wrinkling factor due to intrinsic instability. The model is based on the grid value of n_c representing the number of unstable wavelengths inside the LES filter size. Such model has been shown to adequately perform on a wide range of filter sizes by means of an a-priori analysis and a strategy to include the proposed model in a turbulent combustion closure has also been discussed.

Acknowledgments

The authors acknowledge CINECA for computing resources (IscrB-DNS-LS grant).

Reference

[1] M. Matalon, Annu. Rev. Fluid Mech. 39 (2007) 163–191.

[2] M. Frankel, G. Sivashinsky, Combust. Sci. Technol. 29 (3-6) (1982) 207–224.

[3] P. Pelce, P. Clavin, J. Fluid Mech. 124 (1982) 219–237.

[4] M. Matalon, B. Matkowsky, J. Fluid Mech. 124 (1982) 239–259.

[5] M. Matalon, C. Cui, J. Bechtold, J. Fluid Mech. 487 (2003) 179–210.

[6] P. E. Lapenna, R. Lamioni, G. Troiani, F. Creta, Proc. Combust. Inst. 37 (2) (2019) 1945–1952.

[7] C. Almarcha, B. Denet, J. Quinard, Combust. Flame 162 (4) (2015) 1225–1233.

[8] G. Troiani, F. Creta, M. Matalon, Proc. Combust. Inst. 35 (2) (2015) 1451–1459.

[9] S. Yang, A. Saha, Z. Liu, C. K. Law, Jour. Fluid Mech. 850 (2018) 784–802.

[10] B. Denet, P. Haldenwang, Combust. Sci. and Technol. 104 (1-3) (1995) 143–167.

[11] B. Denet, Phys. Rev. E 55 (6) (1997) 6911.

[12] F. Creta, M. Matalon, Jour. Fluid Mech. 680 (2011) 225–264.

[13] R. Yu, X. S. Bai, V. Bychkov, Phys. Rev. E 92 (6) (2015) 063028.

[14] C. E. Frouzakis, N. Fogla, A. G. Tomboulides, C. Altantzis, M. Matalon, Proc. Combust. Inst. 35 (1) (2015) 1087–1095.

[15] L. Berger, K. Kleinheinz, A. Attili, H. Pitsch, Proc. Combust. Inst. 37 (2) (2019) 1879–1886.

[16] S. Kadowaki, T. Hasegawa, Prog. Energy Combust. Sci. 31 (3) (2005) 193–241.

[17] C. Altantzis, C. Frouzakis, A. Tomboulides, M. Matalon, K. Boulouchos, J. Fluid Mech. 700 (2012) 329–361.

[18] S. Yang, A. Saha, F. Wu, C. K. Law, Combust. Flame 171 (2016) 112–118.

[19] D. Fernández-Galisteo, V. N. Kurdyumov, P. D. Ronney, Combustion and Flame 190 (2018) 133–145.

[20] V. A. Sabelnikov, A. N. Lipatnikov, Ann. Rev. Fluid Mech. 49 (2017) 91–117.

[21] V. Molkov, D. Makarov, A. Grigorash, Combust. Sci. and Technol. 176 (5-6) (2004) 851–865.

[22] R. Keppeler, M. Pfitzner, Combust. Theor. Model. 19 (1) (2015) 1–28.

[23] C. K. Law, G. Jomaas, J. K. Bechtold, Proc. Combust. Inst. 30 (1) (2005) 159–167.

[24] J. Yuan, Y. Ju, C. K. Law, Proc. Combust. Inst. 31 (1) (2007) 1267–1274.

[25] C. Cohé, F. Halter, C. Chauveau, I. Gökalp, Ö. L. Gülder, Proc. Combust. Inst. 31 (1) (2007) 1345–1352.

[26] M. Klein, D. Alwazzan, N. Chakraborty, Computers & Fluids 173 (2018) 178–188.

[27] F. Halter, C. Chauveau, I. Gökalp, International Journal of Hydrogen Energy 32 (13) (2007) 2585–2592.

[28] N. Chakraborty, M. Klein, Phys. Fluids 20 (8) (2008) 085108.

[29] F. Creta, R. Lamioni, P. E. Lapenna, G. Troiani, Phys. Rev. E 94 (5) (2016) 053102.

[30] R. Lamioni, P. E. Lapenna, G. Troiani, F. Creta, Flow Turb. Combust. 101 (4) (2018) 1137–1155.

[31] R. Lamioni, P. E. Lapenna, G. Troiani, F. Creta, Proc. Combust. Inst. 37 (2) (2019) 1815–1822.

[32] P. E. Lapenna, F. Creta, J. Sup. Fluids 128 (2017) 263–278.

[33] P. E. Lapenna, R. Lamioni, P. P. Ciottoli, F. Creta, AIAA-paper 2018-0346.

[34] P. E. Lapenna, Phys. Fluids 30 (7) (2018) 077106.

[35] P. E. Lapenna, F. Creta, AIAA Jour. 57 (6) (2019) 2254–2263.

[36] P. F. Fischer, J. W. Lottes, S. G. Kerkemeier, nek5000 web page, http://nek5000.mcs.anl.gov.

[37] A. T. Patera, J. Comput. Phys. 54 (3) (1984) 468–488.

[38] M. Klein, N. Chakraborty, S. Ketterl, Flow Turb. Combust. 99 (3-4) (2017) 955–971.

[39] G. I. Sivashinsky, Acta Astronautica 4 (1977) 1177–1206.

[40] F. Creta, N. Fogla, M. Matalon, Combust. Theo. Model. 15 (2) (2011) 267–298.

[41] V. V. Bychkov, Phys. Fluids 10 (8) (1998) 2091–2098.

[42] S. Chaudhuri, V. Akkerman, C. K. Law, Phys. Rev. E 84 (2) (2011) 026322.

[43] M. Boger, D. Veynante, H. Boughanem, A. Trouvé, in: Symp. (Int.) Combust., Vol. 27, Elsevier, 1998, pp. 917–925.

[44] M. Klein, N. Chakraborty, Combust. Sci. Technol. 191 (1) (2019) 95–108.

Subgrid modeling of intrinsic instabilities in premixed flame propagation

Pasquale Eduardo Lapenna[ab], Rachele Lamioni[a], Francesco Creta[a]

[a] *Dept. of Mechanical and Aerospace Engineering, Sapienza University of Rome, Italy*
[b] *ENEA C.R. Casaccia, via Anguillarese 301, Rome, Italy*

Abstract

This work is devoted to the investigation and subgrid-scale modeling of intrinsic flame instabilities occurring in the propagation of a deflagration wave. Such instabilities, of hydrodynamic and thermodiffusive origin, are expected to be of particular relevance in recent technological trends such as in the use of hydrogen as a clean energy carrier or as a secondary fuel in hydrogen enriched combustion. A dedicated set of direct numerical simulations is presented and used, in conjunction with coherent literature results, in order to develop scaling arguments for the propagation speed of self-wrinkled flames which are also supported by the outcomes of a weakly non-linear model. The observed scaling is based on the number of unstable wavelengths in a planar flame and is used to develop an algebraic model for the wrinkling factor in the context of a flame surface density closure approach. An a-priori analysis shows that the model correctly captures the flame wrinkling caused by intrinsic instability at sub grid level. A strategy to include the developed self-wrinkling model in the context of a turbulent combustion model is finally discussed on the basis of the turbulence induced cut-off concept.

Keywords: Intrinsic flame instability; Darrieus-Landau instability; Thermal-diffusive instability; Direct Numerical Simulation; Wrinkling factor.

Paper length: 6.5 pages including reference according to the two-column format.

Colloquium 1: Laminar Flames

Colloquium 2: Turbulent Flames

Email address: pasquale.lapenna@uniroma1.it, pasquale.lapenna@enea.it, pasquale.lapenna@gmail.com (Pasquale Eduardo Lapenna[a])

1. Introduction

Intrinsic instabilities appear in premixed flames in different forms and scales [1]. The two intrinsic mechanisms are the Darrieus-Landau (DL) or hydrodynamic instability caused by the thermal expansion and the thermodiffusive (TD) instability generated by unbalanced heat and mass fluxes in the reaction region [2–4]. While the former is ubiquitous and always destabilizing, the latter can be either stabilizing or destabilizing depending on the effective Lewis number of the controlling reactant [5]. The DL instability can only develop for large-scale flames as the scale of its induced wrinkling is typically two orders of magnitude larger than flame thickness in both laminar as well as turbulent settings [6]. The DL features have been studied both experimentally [7–9] and numerically, employing techniques ranging from weakly non-linear models to direct numerical simulations (DNS) [10–13]. Conversely, TD instability manifests itself typically in lean hydrogen flames, with small scale cellular structures on the order of some flame thicknesses as shown by DNS [14–17] as well as experiments [18, 19].

From a phenomenological standpoint, a flame which is intrinsically unstable, tends to propagate faster than its corresponding stable case. The DL or TD induced corrugations in its nonlinear evolution tends to increase the instantaneous flame area and therefore the mean propagation of the entire flame front creating a self-turbulent propagation regime, even in the absence of any incoming turbulence [20]. The modeling of the self-wrinkling behavior as well as the interplay of instabilities and turbulence still require a substantial research effort. In fact, state-of-the-art premixed combustion models do not include any instability-related parameter: see for instance the discussion on flame surface density (FSD) in [6]. Nevertheless, some attempts have been made, in the context of sub grid scale (SGS) modeling for large eddy simulations (LES) of unconfined deflagration [21] and Bunsen flames[22].

This being said, the investigation of intrinsic instability is nowadays also of practical importance, being motivated by recent technological trends such as the increasing operating pressure of combustion chambers as well as the use of hydrogen as a clean energy carrier or as a secondary fuel in hydrogen enriched flames. These conditions are expected to promote the occurrence of both TD and DL instability [23–26], creating challenging conditions to model turbulent premixed combustion, which can lead to non-predictive results from standard approaches: see for instance [27]. In this framework, the present work aims at the analysis and modeling of the flame wrinkling ensuing from intrinsic flame instabilities. To this end, a DNS dataset consisting of two series of flames influenced by DL and TD instability is developed without any turbulent forcing. The ensuing mean propagation speeds, in conjunction with similar results from recent DNS works [13–15], are used to develop an algebraic wrinkling factor model. Such model is tested in an a-priori fashion following [28]. Finally the possibile inclusion of the model into turbulent combustion closure based on the FSD concept, is discussed.

2. Theoretical and numerical framework

2.1. The lengthscales of intrinsic instabilities

In the context of intrinsic instabilities, linear stability analysis of a planar flame is a viable technique to estimate the lengthscales at play. The ensuing dispersion relation $\omega(k)$, where ω is the growth rate of a small perturbation of wavelength λ and wavenumber $k = 2\pi/\lambda$, furnishes two reference lenghtscales, namely the cutoff (or neutral) wavelength $\lambda_c = 2\pi/k_c$, where $\omega(k_c) = 0$ and the most unstable wavelength λ_{max} for which $d\omega/dk = 0$. Such lenghtscales as well as the shape of $\omega(k)$ are largely influenced by the Lewis number of the fuel Le as shown in Fig. 1, in which dispersion relations have been obtained numerically by means of DNS, using the approach described later. As Le decreases, k_c becomes larger and around $Le \approx 0.6$, the dispersion relation exhibits an overshoot above the linear behavior representing the DL mechanism. This indicates that below a critical Lewis number Le_0, thermal-diffusive effects are destabilizing for the flame front [5]. For $Le > Le_0$ i.e. when thermal-diffusive effects are stabilizing, dispersion relations can be either reconstructed numerically by means of DNS or determined analytically using variable fidelity hydrodynamic models [4, 5]. Conversely, for $Le < Le_0$ i.e. for destabilizing thermal-diffusive effects, analytical models are not available and $\omega(k)$ can only be obtained numerically as in Fig. 1.

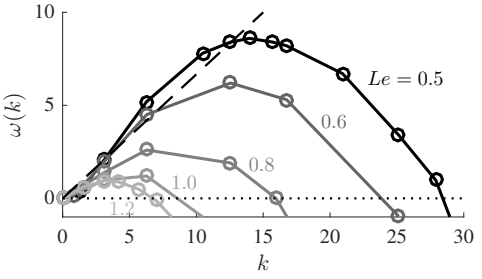

Figure 1: Lewis number effect on the dispersion relation

As discussed in [6], λ_c thus acquires the meaning of a characteristic flame lengthscale, on equal foot-

ing with flame thickness to be compared to turbulence lenghtscales. Indeed λ_c is uniquely defined by the thermochemical conditions, such as the unburned flame temperature T_u, background pressure p_0 and mixture ratio ϕ. A measure of the degree of instability is given by $n_c = L/\lambda_c$, the number of unstable wavelengths within a reference hydrodynamic length L, which is assumed as the largest lengthscale constraining the flame. The higher the value of $n_c > 1$, the larger the number of unstable cells and the more severe the corrugation of the flame is to be expected.

2.2. *DNS datasets*

Intrinsically unstable flames are typically very large scale flames [6] and their DNS requires long simulation times [15]. The computational cost of large scale flame simulations is elevated even in 2D settings with simple chemistry, which are indeed used in this work. In order to have a dataset capable of sustaining scaling arguments with good confidence, we employ, in addition to our DNS data, coherent results from other groups. Our simulations employ a well established framework [6, 29–31], based on the low-Mach number approximation and on a deficient reactant controlling a one-step irreversible reaction. This approach is implemented in an equation-of-state-independent version [32–35] of the highly-efficient parallel code *nek5000* [36] based on the spectral element method (SEM) [37].

Two series of planar flames have been simulated, designated TD and DL to highlight respectively the presence or absence of thermal-diffusive instabilities, with increasing values of n_c. For each simulation λ_c, needed to determine n_c, has been evaluated numerically and, where possible, compared to analytical dispersion relations [5]. The computational domain is periodic in the crosswise direction while outflow conditions are imposed at the upper boundary in the streamwise direction. Statistically planar flames are obtained by means of an inflow/outflow configuration, imposing the instantaneous burning velocity as the inflow velocity at the lower boundary [38] without introducing any turbulent perturbation. The SEM discretization is uniform and the resolution chosen in order to have, for the less resolved case, at least 14 grid points within the thermal thickness of a 1D unstretched flame, defined as $\delta_T = (T_b - T_u)/\max(dT/dx)$. The simulations are initialized by means of a 1D flame with the superimposition of a small broadband velocity disturbance to trigger the instability and statistics are collected only after reaching the non-linear regime.

The TD series is characterized by a ratio between the domain width and the flame thickness L/ℓ_D ranging from 40 up to 400, resulting in a wide range of n_c. The size of the computational domain in the streamwise direction L_y is two times the periodic dimension L, which was verified to be large enough to correctly contain the corrugated flame for the entire non-linear evolution studied. Conversely, the DL series is obtained by varying both the expansion ratio σ and the Lewis number Le while keeping constant $L/\ell_D = 400$. In this series a computational domain in the streamwise direction of $L_y = L$ was deemed large enough, except for the simulation labeled as DL3 in which $L_y = 2L$. As a result, being λ_c larger in units of ℓ_D for thermal-diffusively stable flames, the range of n_c that can be explored by the DL series using similar computational resources is clearly narrower than the TD series. A summary of the DNS parameters is reported in table 1 in conjunction with the mean propagation speeds S_T/S_L^0 while instantaneous realizations of the largest flames, namely TD3 and DL3, are displayed in Fig. 2. We also employ literature data from other recent DNS simulations of two-dimensional, self-turbulent flames. In particular, mean propagation speed of statistically planar flames are taken from the following: (i) Yu et al. [13], hydrodynamically unstable one-step chemistry flames with $Le = 1$, $\sigma = 5, 8, 10$

Table 1: Summary of DNS parameters and characteristics.

Label	Le	σ	Ze	n_c	L/ℓ_D	S_T/S_L^0
DL1	1.36	10.0	8.0	9.2	400	1.57
DL2	1.00	6.67	8.0	13.7	400	1.32
DL3	1.00	10.0	8.0	16.3	400	1.85
TD1	0.49	6.67	8.0	7.6	40	2.03
TD2	0.49	6.67	8.0	20.0	105	4.03
TD3	0.49	6.67	8.0	76.0	400	4.52

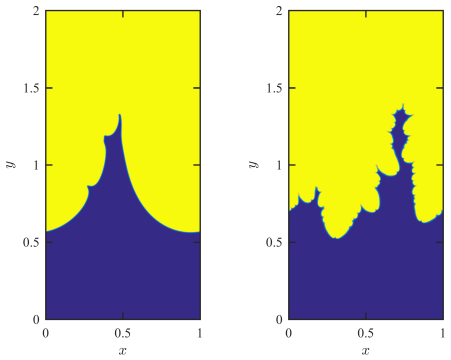

(a) DL3 (b) TD3

Figure 2: Progress variable fields for the largest flames of the dataset. Color code from blue ($c = 0$ unburnt) to yellow ($c = 1$ burnt).

and $n_c = 1 - 95$; (ii) Berger et al. [15], TD unstable, lean hydrogen flames ($\phi = 0.44$) at an estimated effective Lewis number of $Le = 0.39$ and $\sigma = 4.4$ data taken only in the range $n_c = 2-300$; (iii) Frouzakis et al. [14], TD unstable lean hydrogen flames ($\phi = 0.5$, estimated $Le = 0.53$ and $\sigma = 5$) in the range $n_c = 2 - 4$.

3. Results and discussion

3.1. Analysis and modeling of self-wrinkling

Phenomenologically, the self wrinkling caused by intrinsic flame instability is associated to a flame area increase responsible for the overall flame speed enhancement. Any attempt to model such wrinkling should involve the determination of a scaling law for S_T/S_L^0 and the adequate set of independent parameters governing it. Valuable information can be obtained from the Sivashinsly equation [39], modeling the unsteady perturbation $u(x,t)$, about the nominal planar conformation, of a potentially hydrodynamically and thermodiffusively unstable flame with weak thermal expansion. The integrodifferential model in a periodic domain of size L is originally cast as a function of the expansion ratio σ and of a parameter ϵ measuring the deviation of the Lewis number from the critical value Le_0. This can be reduced through variable transformation to a one parameter equation in one spatial dimension:

$$u_t + u_{xxxx} + \beta u_{xx} + 1/2 u_\xi^2 = I(u) \qquad (1)$$

where β is the only surviving parameter and $I(u)$ is the non-local Hilbert transform of the derivative of u representing thermal expansion effects. As β is varied, the enhanced propagation speed of a cellular flame, solution of the model, is obtained by time averaging the flame area. Noting that the associated dispersion relation depends on the unique parameter β, so will the suitably rescaled cutoff wavelength λ_c' and rescaled number of unstable wavelengths n_c'. One thus expects the averaged propagation speed to exhibit a universal scaling law as a function of n_c'. This is indeed the case as shown in Fig. 3 displaying, for a large number of solutions, the incremental propagation speed $[(S_T/S_L^0) - 1]$ rescaled by $(1-\sigma^{-1})^2$ to compensate for thermal expansion which tends to increase the amplitude of corrugations. For small values of $n_c' > 1$ one observes flame conformations similar to *pole* solutions (0.125 asymptotic value) [40] typical of DL instability, while for larger n_c' additional wrinkling due to growing effects of TD instability further increases the propagation speed.

On the basis of the indications gleaned through the Sivashinsky model, it is reasonable to scale the averaged burning velocity from the DNS database as a function of: (i) n_c, as a measure of the degree of intrinsic instability and (ii) σ, to account for the effect of thermal expansion on the amplitude of the corrugation. To compensate for thermal expansion, we employ this time the function $U_m(\sigma)$, in lieu of $(1 - \sigma^{-1})^2$, derived for realistic values of σ by Bychkov [41], representing the incremental propagation speed of a corrugated stationary flame subject to DL instability. Such function, was verified against dedicated DNS data, although we do not show this for brevity. Figure 4 finally shows the rescaled incremental propagation speed $(S_T/S_L^0 - 1)/U_m$, as a function of n_c. It is clearly noticeable that flames influenced by TD instability propagate faster, for a given n_c, than the purely hydrodynamically unstable flames. The latter ($Le > Le_0$) seem to follow reasonably well the analytical incremental propagation speed of pole solutions $U_N(n_c) = \frac{1}{2}\frac{N}{n_c}(1-\frac{N}{n_c})$ with $N = \mathrm{int}(n_c/2+1/2)$ [41]. This trend remains valid up to a secondary cutoff limit, that can be identified between n_c values of 4-4.5 [42] and 7-8 [13], when the well-known global steady DL structure becomes again unstable as the large scale flame starts behaving as a set of quasi-planar, smaller scale unstable flames [42] exhibiting additional wrinkling and a fractal conformation [13, 40]. This additional wrinkling is also present in the simulations DL1-3 from this study, and clearly shown for DL3 case in Fig.2. However, in the case of extremely large domains L, namely more than 2 orders of magnitude larger than λ_c ($n_c > 100$), it is still unclear if a domain independence will be reached. Conversely, for TD unstable flames ($Le < Le_0$) a plateau is reached beyond $n_c \sim 30$ with the largest DNS presented in this work, namely the TD3 case shown in Fig. 2 that confirms the trend recently explained by Berger et al. [15]. On the other hand smaller flames, $n_c \sim 2 - 30$, show a steady increase before reaching the mentioned plateau.

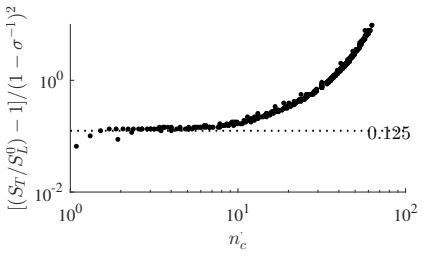

Figure 3: Incremental propagation speed obtained averaging the solutions of the Sivashinsly equation.

The foregoing observations on propagation speed in the presence of intrinsic instabilities suggest a possible modeling strategy in the context of the generalized FSD approach [43]. The generalized FSD $\Sigma_{\mathrm{gen}} = \overline{|\nabla c|}$ can be modeled by introducing an algebraic expression for the

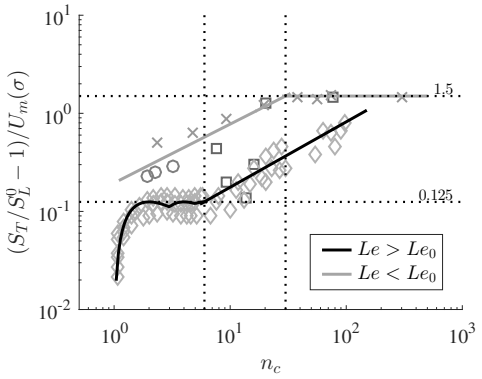

Figure 4: Rescaled incremental propagation speed $(S_T/S_L^0 - 1)/U_m$ plotted against n_c: diamonds (◇) Yu et al. data [13], crosses (×) Berger et al. data [15], circles (◯) Frouzakis et al. data and squares (□) this study. Continuos lines represent wrinkling factor models in the presence of intrinsic instability for TD and DL cases.

wrinkling factor $\Xi = \overline{|\nabla c|}/|\nabla \overline{c}|$, representing the effect of subgrid wrinkling [28, 43]. In the present context of laminar, self-corrugated, unstable flames, the wrinkling factor can be directly related to flame speed, i.e. $\Xi_L \sim S_T/S_L^0$. This suggests that the rescaled propagation speed of Fig. 4 can be used directly to model the wrinkling factor in a data-driven fashion. Indeed we can conjecture that in a generic setting of turbulent propagation, the overall wrinkling factor Ξ will be a function of both the intrinsic laminar wrinkling Ξ_L and the standard contribution of the turbulent wrinkling Ξ_T. The continuous lines shown in Fig. 4, fitting the DNS data with a $\sim 20\%$ mean error, can thus effectively represent the model $\Xi_L \sim S_T/S_L^0$, as summarized in Tab. 2.

Table 2: Wrinkling factor model Ξ_L for TD and DL flames.

Le range	n_c range	model expression
any	$n_c < 1$	$\Xi_L = 1$
$Le > Le_0$	$n_c < 6$	$\Xi_L = 1 + U_m(\sigma)(U_N(n_c))$
	$n_c > 6$	$\Xi_L = 1 + U_m(\sigma)(.04 n_c^{2/3})$
$Le < Le_0$	$n_c > 1$	$\Xi_L = 1 + U_m(\sigma)(.19 n_c^{3/5})$
	$n_c > 30$	$\Xi_L = 1 + U_m(\sigma)(1.5)$

Note that for $n_c < 1$ all models should collapse on $\Xi_L = 1$ as the flame is stable within the hydrodynamic domain of interest. Different ranges on n_c are introduced due to the additional cut-off values previously discussed for both TD and DL instability.

The concept of n_c in the context of SGS models should be further explored. The definition of $n_c = L/\lambda_c$ expresses the number of unstable wavelengths within the hydrodynamic length L. In a RANS context, where all the instability-induced wrinkling is unresolved, we should consider L as being the reference hydrodynamic length (e.g. a Bunsen or injector diameter). As a result, n_c is generally expected to be large, thus yielding correspondingly non-unity values of Ξ_L. On the other hand, in an LES context, a portion of the wrinkling may well be resolved on the grid, implying that the hydrodynamic length should be considered as the local grid size $L = \Delta$ so that $n_c = \Delta/\lambda_c$. For $Le > Le_0$ mixtures (such as rich hydrocarbon mixtures), λ_c can be assumed to be of the order of 10^2 flame thicknesses [6], thus making it extremely likely that $n_c = O(1)$ or less (unless $\Delta > 10^2$ flame thicknesses or larger), thus not requiring any modeling. Conversely, for $Le < Le_0$ (such as lean hydrogen mixtures) λ_c is generally far smaller and can be assumed to be of the order of $10\delta_T$ or less [15], such as in the present TD series of DNS where $\lambda_c \sim 4\delta_T$. This entails a possible value for $n_c > 1$ if the LES filter width is some flame thicknesses wide, which is a far more likely scenario. This reasoning shows that LES of hydrogen or hydrogen-diluted flames may likely require SGS modeling for the unresolved instability-induced wrinkling as confirmed by the a-priori analysis in the next subsection. This being said, whether in a RANS or LES context, a global or local value of n_c should invariably be determined, for the given fuel mixture and given geometry or grid. A good practice would thus require the determination of λ_c for the given mixture and conditions, by numerically determining the flame's dispersion relation.

3.2. A priori analysis of the proposed model

The proposed modeling strategy based on Ξ_L, is now a-priori tested by filtering DNS data using a Gaussian shaped kernel. The overbar $\overline{\cdot}$ denotes LES filtering and the assessment of the FSD based modeling strategy follows standard criteria [28]: (1) the total modeled flame surface area, i.e. the volume-averaged generalized FSD $\langle \Sigma_{gen} \rangle$, should be equal to the DNS value and as independent as possible from Δ; (2) the statistical correlation between the modeled Σ_{gen} and the DNS value should be close to unity, (3) the model should be able to capture the correct variation of conditionally averaged values of Σ_{gen} with filtered reaction progress variable across the flame brush. The two largest simulations of the dataset, namely DL3 and TD3, are filtered using a wide range of filter sizes from $\Delta = \Delta_{DNS}$ up to $\Delta = 40\delta_T$.

Figure 5 displays the capabilities of $\Sigma_{gen} = \Xi_L |\nabla \overline{c}|$ of reproducing the total flame surface area obtained from the DNS (criterion 1). An overall agreement between the model and the DNS data is observed. In the DL case, the model shows an under-prediction throughout the filter sizes explored. In particular we have $\Xi_L = 1$ until $\Delta \sim \lambda_c \sim 13\delta_T$ where n_c becomes greater than

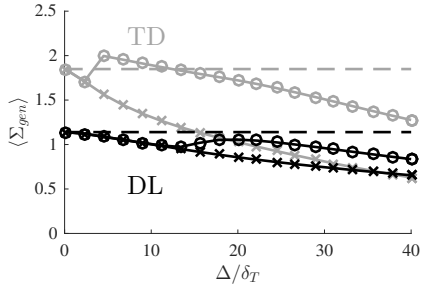

Figure 5: Total volume-averaged value of the generalized FSD as a function of the filter width: DNS value (dashed lines, −−), modeled Σ_{gen} (circles, ◯) and resolved part of the FSD $|\nabla\overline{c}|$ (crosses, ×).

unity. For $\Delta/\delta_T > 13$ the wrinkling factor $\Xi_L > 1$ reduces the difference between $\Xi_L|\nabla\overline{c}|$ and the DNS value. Note that, even for the largest filter size $\Delta/\delta_T \sim 40$, the second part of the model, which activates for n_c greater than the secondary cut-off, was never utilized. Such region would have been explored if Δ were large enough to accommodate at SGS level a large enough flame to exhibit a fractal-like wrinkling. However, such large size filters, compared to the instability and flame length-scales, cannot be expected in a turbulent scenario as this would imply unrealistically low-Karlovitz numbers, see e.g. Fig.2 of [6]. In the TD case, the model activates at a smaller Δ, around $\Delta/\delta_T \sim 4$, causing a temporary over-prediction of $\langle\Sigma_{gen}\rangle$ until $\Delta/\delta_T \sim 13$. To some extent, this is a good scenario for the interaction between modeling strategies and numerical errors in LES [44]. In addition, the largest filter size $\Delta/\delta_T \sim 40$ is characterized by $n_c \sim 12$ and, as a result, also in this case the second part of model has not been explored. Nonetheless, contrary to DL flames, for TD unstable flames the plateauing region of the Ξ_L model could be realistically used in an LES of a sufficiently large scale flame.

In order to further test the model we now focus on three filter sizes $\Delta/\delta_T \sim 5, 15, 30$ namely fine, medium and coarse. The effect of Δ on c-fields of the TD3 and DL3 cases are shown in Fig.6. It is clearly observable that the secondary wrinkling of the DL case is resolved on the fine grid while for the coarse it is undetectable as the only structure resolved is the large scale DL cusp. In the TD case, the small scale wrinkling is barely visible on the fine grid and undetectable on others, conversely large scale flame fingers are resolved on both fine and medium grids, while at the largest Δ it starts being undetected. As a partial conclusion, in an LES setting, large scale features of both TD and DL type flames can be considered always resolved on the computational grid.

The model is further assessed by investigating the conditionally averaged values of Σ_{gen} to $\overline{c}$ (criterion 3).

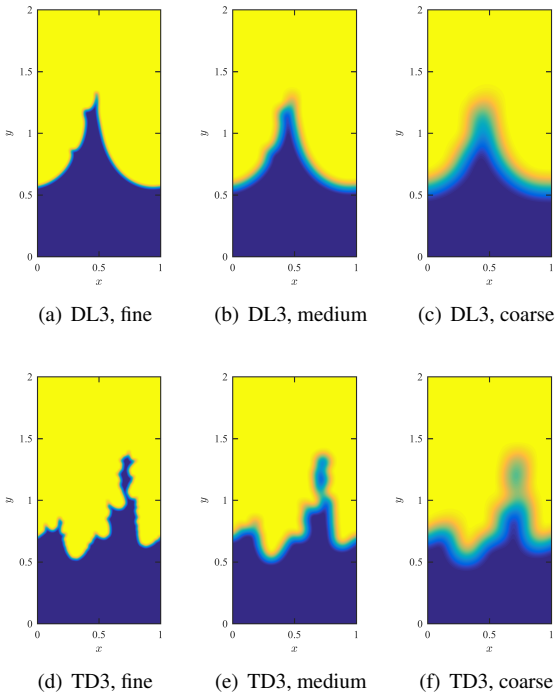

(a) DL3, fine (b) DL3, medium (c) DL3, coarse

(d) TD3, fine (e) TD3, medium (f) TD3, coarse

Figure 6: The effect of filtering on the instantaneous realizations displayed in Fig. 2: left column TD3 case, right column DL3 case.

These quantities are displayed in Fig. 7 showing that the model can reproduce both in shape and magnitude the DNS data. Moreover, Fig. 7 also reports the correlation coefficient between the modeled Σ_{gen} and DNS values (criterion 2), which remain sufficiently close to unity. For the DL flame, Fig. 7(a) and 7(c) statistically confirm the conclusions drawn by observing the $\overline{c}$ fields as $\Xi_L \to 1$ for the medium and fine grid. Only using a large Δ, Ξ_L is appreciably higher than unity and its effect on Σ_{gen} clearly visible. Indeed, for such filter size, the secondary DL structures are statistically not resolved on the mesh. On the other hand, in this case the Σ_{gen} of the DNS is slightly skewed towards the burnt gas side and not perfectly reproduced by the model for $\overline{c} > 0.4$. For the TD flame, the scenario is completely different since the small scale wrinkles require modeling in both the medium and fine grids and the model correctly captures the DNS data across the entire flame brush. In the coarse mesh case, similarly to the DL flame, the exact Σ_{gen} is slightly skewed toward $\overline{c} = 1$ and the model perfectly reproduces the DNS data for $\overline{c} < 0.5$.

3.3. Extension to the turbulent case

A final note is dedicated to the extension of the model of Tab. 2 to a realistic turbulent scenario. Indeed, we recall that such model was derived in a self-wrinkling

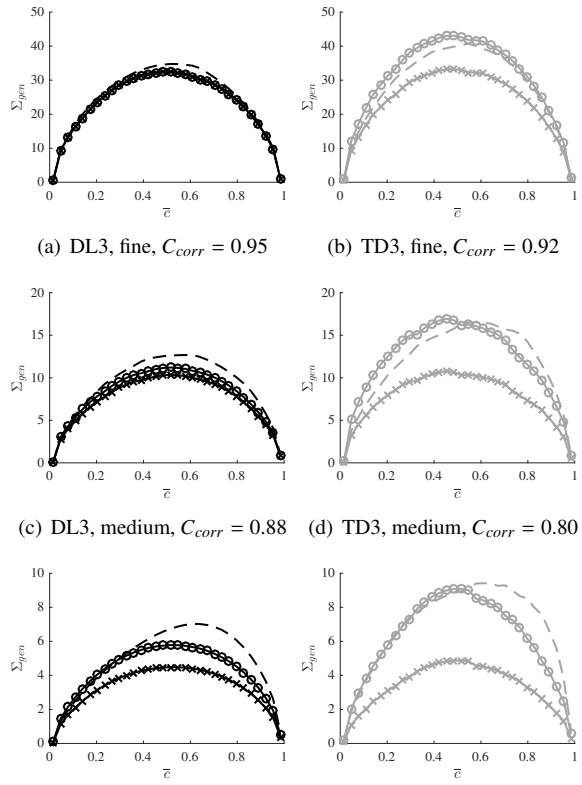

(a) DL3, fine, $C_{corr} = 0.95$ (b) TD3, fine, $C_{corr} = 0.92$

(c) DL3, medium, $C_{corr} = 0.88$ (d) TD3, medium, $C_{corr} = 0.80$

(e) DL3, coarse, $C_{corr} = 0.79$ (f) TD3, coarse, $C_{corr} = 0.72$

Figure 7: Conditionally averaged values of $\Sigma_{gen} = \Xi_L|\nabla\overline{c}|$ to $\overline{c}$, using the three filters $\Delta/\delta_T \sim 5, 15, 30$ namely fine, medium and coarse: DNS (dashed lines, $--$), modeled Σ_{gen} (circles, ◯) and resolved part of the generalized FSD $|\nabla\overline{c}|$ (crosses, ×). Also reported for each case the correlation coefficient C_{corr} between the exact and modeled Σ_{gen}.

setting and its characteristics may vary in a turbulent scenario. Previous studies have shown [29, 31], albeit limited to $Le > Le_0$, that for increasing turbulence intensity, the effects of instability-induced wrinkling tend to be mitigated. This may suggest that at high turbulence intensity, the model may have a reduced or even vanishing effect ($\Xi_L \to 1$). Therefore, to tentatively introduce the mitigation of instability, it is of interest to use the concept of turbulence-induced DL cutoff $\tilde{\lambda}_c$, a function of turbulence and instability parameters [42].

A simple way to incorporate turbulence effects is to define a *turbulent* n_c based on the filter size and $\tilde{\lambda}_c$ as $\tilde{n}_c = \Delta/\tilde{\lambda}_c$. The overall wrinkling factor model can be expressed as $\Xi = \Xi_L(\tilde{n}_c, \sigma)\Xi_T$ where $\Xi_L(\tilde{n}_c, \sigma)$ is the model of Tab. 2 using $\tilde{n}_c$ in lieu of the laminar value, while Ξ_T is a standard model for turbulent premixed combustion. In the limit case of a laminar setting $\tilde{n}_c \to n_c$ while for elevated turbulence intensity $\tilde{n}_c \to 0$ resulting in $\Xi_L = 1$. This being said, the effectiveness of this extension is based on a proper estimation of $\tilde{\lambda}_c$ that defines $\tilde{n}_c$ on the LES grid. While for DL flames the definition in [42] could be tested, for TD flames it still remains to be investigated/proposed. It is not known, in fact, whether this mitigation effect will also occur for $Le < Le_0$, where it may be delayed by the small scale and persistent nature of thermal-diffusive corrugations.

4. Conclusion

The propagation of intrinsically unstable flames has been investigated and a model to incorporate the possibile occurrence of instability-induced wrinkling at subgrid level has been introduced. The model is based on scaling arguments of the average propagation speed as a function of the number of unstable wavelengths for a planar premixed flame n_c. The scaling has been sustained by the results of a weakly non-linear model and by the development of a dedicated DNS dataset as well as other coherent literature results. In particular, purely hydrodynamically unstable flames seem to exhibit incremental propagation speeds which follow quite well analytical pole solutions until reaching the secondary cut-off value beyond which additional wrinkling appears. Conversely, thermodiffusively unstable flames show a different scaling with n_c leading to incremental propagation speeds which are larger than for the corresponding purely hydrodynamic case, eventually reaching a plateau at a large scale cut-off value. The ensuing data have been used to introduce an algebraic model for the wrinkling factor due to intrinsic instability. The model is based on the grid value of n_c representing the number of unstable wavelengths inside the LES filter size. Such model has been shown to adequately perform on a wide range of filter sizes by means of an a-priori analysis and a strategy to include the proposed model in a turbulent combustion closure has also been discussed.

Acknowledgments

The authors acknowledge CINECA for computing resources (IscrB-DNS-LS grant).

Reference

[1] M. Matalon, Annu. Rev. Fluid Mech. 39 (2007) 163–191.
[2] M. Frankel, G. Sivashinsky, Combust. Sci. Technol. 29 (3-6) (1982) 207–224.
[3] P. Pelce, P. Clavin, J. Fluid Mech. 124 (1982) 219–237.
[4] M. Matalon, B. Matkowsky, J. Fluid Mech. 124 (1982) 239–259.
[5] M. Matalon, C. Cui, J. Bechtold, J. Fluid Mech. 487 (2003) 179–210.
[6] P. E. Lapenna, R. Lamioni, G. Troiani, F. Creta, Proc. Combust. Inst. 37 (2) (2019) 1945–1952.
[7] C. Almarcha, B. Denet, J. Quinard, Combust. Flame 162 (4) (2015) 1225–1233.

[8] G. Troiani, F. Creta, M. Matalon, Proc. Combust. Inst. 35 (2) (2015) 1451–1459.
[9] S. Yang, A. Saha, Z. Liu, C. K. Law, Jour. Fluid Mech. 850 (2018) 784–802.
[10] B. Denet, P. Haldenwang, Combust. Sci. and Technol. 104 (1-3) (1995) 143–167.
[11] B. Denet, Phys. Rev. E 55 (6) (1997) 6911.
[12] F. Creta, M. Matalon, Jour. Fluid Mech. 680 (2011) 225–264.
[13] R. Yu, X. S. Bai, V. Bychkov, Phys. Rev. E 92 (6) (2015) 063028.
[14] C. E. Frouzakis, N. Fogla, A. G. Tomboulides, C. Altantzis, M. Matalon, Proc. Combust. Inst. 35 (1) (2015) 1087–1095.
[15] L. Berger, K. Kleinheinz, A. Attili, H. Pitsch, Proc. Combust. Inst. 37 (2) (2019) 1879–1886.
[16] S. Kadowaki, T. Hasegawa, Prog. Energy Combust. Sci. 31 (3) (2005) 193–241.
[17] C. Altantzis, C. Frouzakis, A. Tomboulides, M. Matalon, K. Boulouchos, J. Fluid Mech. 700 (2012) 329–361.
[18] S. Yang, A. Saha, F. Wu, C. K. Law, Combust. Flame 171 (2016) 112–118.
[19] D. Fernández-Galisteo, V. N. Kurdyumov, P. D. Ronney, Combustion and Flame 190 (2018) 133–145.
[20] V. A. Sabelnikov, A. N. Lipatnikov, Ann. Rev. Fluid Mech. 49 (2017) 91–117.
[21] V. Molkov, D. Makarov, A. Grigorash, Combust. Sci. and Technol. 176 (5-6) (2004) 851–865.
[22] R. Keppeler, M. Pfitzner, Combust. Theor. Model. 19 (1) (2015) 1–28.
[23] C. K. Law, G. Jomaas, J. K. Bechtold, Proc. Combust. Inst. 30 (1) (2005) 159–167.
[24] J. Yuan, Y. Ju, C. K. Law, Proc. Combust. Inst. 31 (1) (2007) 1267–1274.
[25] C. Cohé, F. Halter, C. Chauveau, I. Gökalp, Ö. L. Gülder, Proc. Combust. Inst. 31 (1) (2007) 1345–1352.
[26] M. Klein, D. Alwazzan, N. Chakraborty, Computers & Fluids 173 (2018) 178–188.
[27] F. Halter, C. Chauveau, I. Gökalp, International Journal of Hydrogen Energy 32 (13) (2007) 2585–2592.
[28] N. Chakraborty, M. Klein, Phys. Fluids 20 (8) (2008) 085108.
[29] F. Creta, R. Lamioni, P. E. Lapenna, G. Troiani, Phys. Rev. E 94 (5) (2016) 053102.
[30] R. Lamioni, P. E. Lapenna, G. Troiani, F. Creta, Flow Turb. Combust. 101 (4) (2018) 1137–1155.
[31] R. Lamioni, P. E. Lapenna, G. Troiani, F. Creta, Proc. Combust. Inst. 37 (2) (2019) 1815–1822.
[32] P. E. Lapenna, F. Creta, J. Sup. Fluids 128 (2017) 263–278.
[33] P. E. Lapenna, R. Lamioni, P. P. Ciottoli, F. Creta, AIAA-paper 2018-0346.
[34] P. E. Lapenna, Phys. Fluids 30 (7) (2018) 077106.
[35] P. E. Lapenna, F. Creta, AIAA Jour. 57 (6) (2019) 2254–2263.
[36] P. F. Fischer, J. W. Lottes, S. G. Kerkemeier, nek5000 web page, http://nek5000.mcs.anl.gov.
[37] A. T. Patera, J. Comput. Phys. 54 (3) (1984) 468–488.
[38] M. Klein, N. Chakraborty, S. Ketterl, Flow Turb. Combust. 99 (3-4) (2017) 955–971.
[39] G. I. Sivashinsky, Acta Astronautica 4 (1977) 1177–1206.
[40] F. Creta, N. Fogla, M. Matalon, Combust. Theo. Model. 15 (2) (2011) 267–298.
[41] V. V. Bychkov, Phys. Fluids 10 (8) (1998) 2091–2098.
[42] S. Chaudhuri, V. Akkerman, C. K. Law, Phys. Rev. E 84 (2) (2011) 026322.
[43] M. Boger, D. Veynante, H. Boughanem, A. Trouvé, in: Symp. (Int.) Combust., Vol. 27, Elsevier, 1998, pp. 917–925.
[44] M. Klein, N. Chakraborty, Combust. Sci. Technol. 191 (1) (2019) 95–108.